Regional Sustainability 4 (2023) 249–260

Contents lists available at ScienceDirect

Regional Sustainability

journal homepage: www.keaipublishing.com/en/journals/regional-sustainability

Full Length Article

Geotechnical and GIS-based environmental factors and vulnerability studies of the Okemesi landslide, Nigeria

Oluwakemi Bolanle Akintan [a], Johnson Adedeji Olusola [a,*], Olaniyi Patrick Imole [a], Moyosoluwa Odunayo Adeyemi [b]

[a] Department of Geography and Planning Science, Ekiti State University, Ado Ekiti, Nigeria
[b] Department of Geology and Mineral Sciences, Crawford University, Igbesa, Ogun State, zip-code, Nigeria

ARTICLE INFO

Keywords:
Rainfall-induced landslide
Landslide hazards
Slope materials
Rainfall
Geomorphology
Vulnerability zone
Okemesi-Ekiti (Okemesi)

ABSTRACT

Landslide is a geological hazard typically associated with extreme events such as earthquakes, heavy rainfall, volcanic eruptions, changes in groundwater level, etc. This study was carried out in Okemesi-Ekiti (also known as Okemesi), Southwest Nigeria, with the purpose of using remote sensing and GIS technologies to analyze the environmental factors (grain size, direct shear strength resistance, rainfall data, wet density, surface, and slope) resulting in the occurrence of the Okemesi landslide. The study also aimed to conduct a vulnerability analysis in the study area to identify regions with a probability of landslide occurrence. The grain size analysis of the soil in the Okemesi landslide area showed that slope materials comprised 17.14% gravel, 59.31% sand, and 19.48% fines, thus the soil type could be classified as poorly graded gravely sand with a high possibility of landslide occurrence. The geomorphic characteristics of the study area was characterized by slopes ranging from 0.00° to 49.00°, while most slopes in the area were less than 8.00°. The slope aspect direction was mainly in south (157.51°–202.50°), southwest (202.51°–247.50°), west (247.51°–292.50°), and north (0.00°–22.50° and 337.51°–360.00°). The highlands were primarily bounded by the slope directions of north (0.00°–22.50° and 337.51°–360.00°), northeast (22.51°–67.50°), east (67.51°–112.51°), and southeast (112.51°–157.50°), which indicated the potential direction of mass movement. The study area can be divided into three vulnerability zones: high, medium, and low, with the area percentages of 9.00%, 61.80%, and 29.20%, respectively. The analysis suggested that the Okemesi landslide was likely triggered by rainfall, which might have weakened the physical structure of slope materials. Understanding the causes and impacts of landslides is crucial for policy-makers to implement measures to mitigate landslide hazards, protect infrastructure, and prevent the loss of life in the landslide-prone regions.

1. Introduction

Landslide is a geological hazard typically associated with extreme events such as earthquakes, heavy rainfall, volcanic eruptions, changes in groundwater level, etc. Whether these events occur alone or in combination, they can potentially damage the slope

* Corresponding author.
E-mail address: johnson.olusola@eksu.edu.ng (J.A. Olusola).

https://doi.org/10.1016/j.regsus.2023.08.001
Received 29 December 2022; Received in revised form 26 May 2023; Accepted 15 August 2023
Available online 21 August 2023

environment (Lee, 2019). According to Bujang et al. (2008) and Gbadebo et al. (2021), rainfall-induced landslide has resulted in deaths, destroyed infrastructure worth billions of dollars, and hampered economic development in many countries around the world. However, over 80.00% of landslide is at least partially caused by human intervention such as poor slope management practices.

Rainfall-induced landslide is one of Nigeria's most recent natural disasters (Ige et al., 2016). Many studies have shown that rainfall intensity or duration, slope material nature, weathering, and permeability are central to rainfall-induced landslide in Nigeria (e.g., Msilimba and Holmes, 2005; Igwe, 2015; Gbadebo et al., 2021). According to Coe (2017), the adequate assessment of climate change activities, particularly rainfall, is critical in the management and mitigation of rainfall-induced landslide. Brand et al. (1984) showed that deeply weathered rocks that form slope materials are prone to down-slope displacement, particularly after prolonged rainfall.

Though landslide can occur anywhere in the world, regional geology, hydrogeology, and geomorphology often determine their mechanisms, impacts, and management measures. Landslide hazards are often localized, implying why mitigation techniques must also take into account the peculiarity (geology, geomorphology, and rainfall) of the landslide; this, however, does not mean there are no universal management measures (Igwe and Una, 2019).

Remote sensing and GIS tools play critical roles in the investigation and zonation of landslide hazards. These tools are useful for the characterization and mapping of landslide. Remote sensing images are not only helpful with acquiring information about past and present local landslide, but also important in identifying landslide hazard zones (Chauhan et al., 2010). Studies such as Ayalew and Yamagishi (2005), Ohlmacher (2007), and Chauhan et al. (2010) have employed landslide mapping zones to assess the influencing factors and sensitive areas of landslide. Quantitative and qualitative approaches are common methods used for evaluating and delineating landslide hazards. In the qualitative method, the experts may assess the landslide susceptibility zones based on their experience. Experts can also predict the vulnerability of the area based on the similar geological and geomorphological characteristics that the area shares with existing landslide (Ayalew and Yamagishi, 2005). Multi-criteria decision is another approach, which uses proper database to accurately identify and determine the potential landslide areas.

Currently, Nigeria has no map or guideline to assess and predict landslide hazards because there is little information about the impact of rainfall on local landslide and slope stability. Equally, predicting the landslide occurrence is difficult without a systematic database of past landslide occurrences, because such predictions require a large amount of data and complex analysis. Ayodele and Odeyemi (2010) and Bamisaiye (2019) have analyzed the Okemesi landslide (Southwest Nigeria) to determine its geotechnical properties. However, this study, in addition to investigating the geotechnical properties of the Okemesi landslide, also applied the tools of remote sensing and GIS to identify the causes of the Okemesi landslide. Moreover, this study differs from the previous studies mentioned above by employing

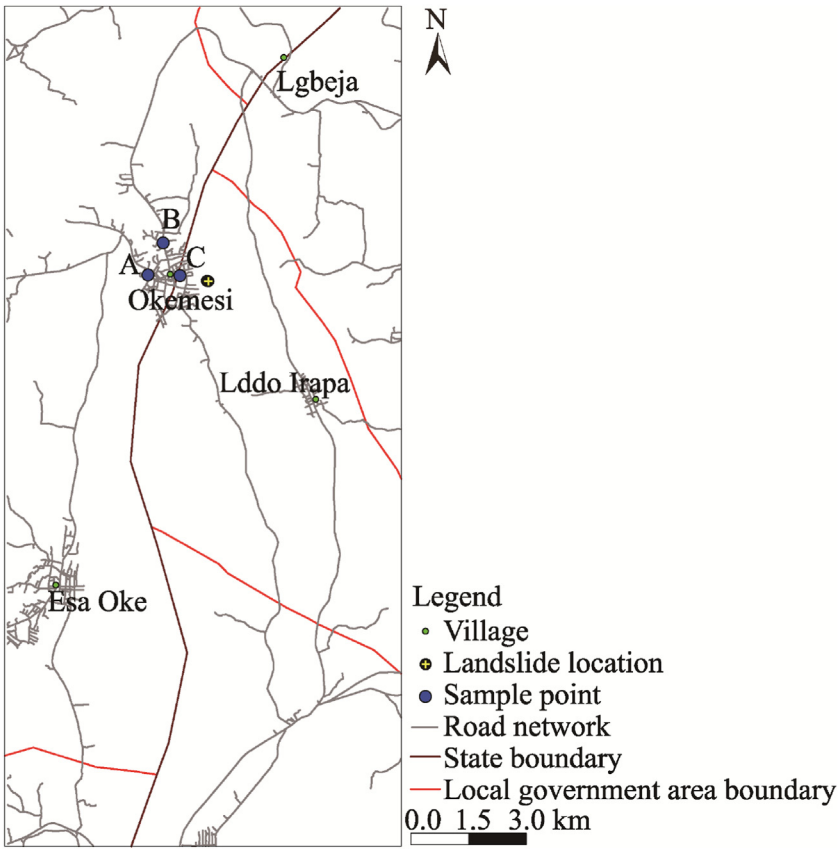

Fig. 1. Overview of the study area and locations of sample points.

remote sensing and GIS tools to investigate how rainfall and other intrinsic and extrinsic factors can trigger landslide. Therefore, the objectives of this study are to identify the geological and geotechnical factors that may trigger the landslide in Okemesi, assess the impacts of landslide on people and communities, and estimate the possibility of future landslide occurrence in the study area. The results of study can provide information to develop guidelines and maps for assessing landslide hazards in Nigeria, develop effective landslide mitigation and prevention strategies, and prepare disaster management plans for subsequent landslide occurrence. This study will fill the knowledge gap regarding the impact of rainfall on landslide and slope instability in Nigeria.

2. Materials and methods

2.1. Study area

Okemesi-Ekiti (also known as Okemesi; 7°50′24″–7°51′00″N, 5°7′12″–5°7′48″E) is a town located in Ijero Local Government Area of Ekiti State, Southwest Nigeria (Fig. 1). According to the 2006 Nigerian Census (National Population Commission of Nigeria, 2016), Okemesi has a population of approximately 16,700. The town is predominantly inhabited by the Yoruba ethnic group. The town has a tropical rainforest climate characterized by high humidity and heavy rainfall, and experiences rainy season from April to October and dry season from November to March of the next year. The topography of the town plays a significant role in the local climate and weather patterns, as well as the occurrence of landslide. The region is also home to a variety of vegetation, including rainforests, grasslands, and agricultural lands.

2.2. Geological setting

The Okemesi fold belt is part of the Ife-Ilesha schist belt, which is the geology of the study area (Fig. 2). The rocks are Southwester part of Nigeria's Pre-Cambrian to Late Proterozoic basement rocks, which are also part of the larger West African Shield (Rahaman,

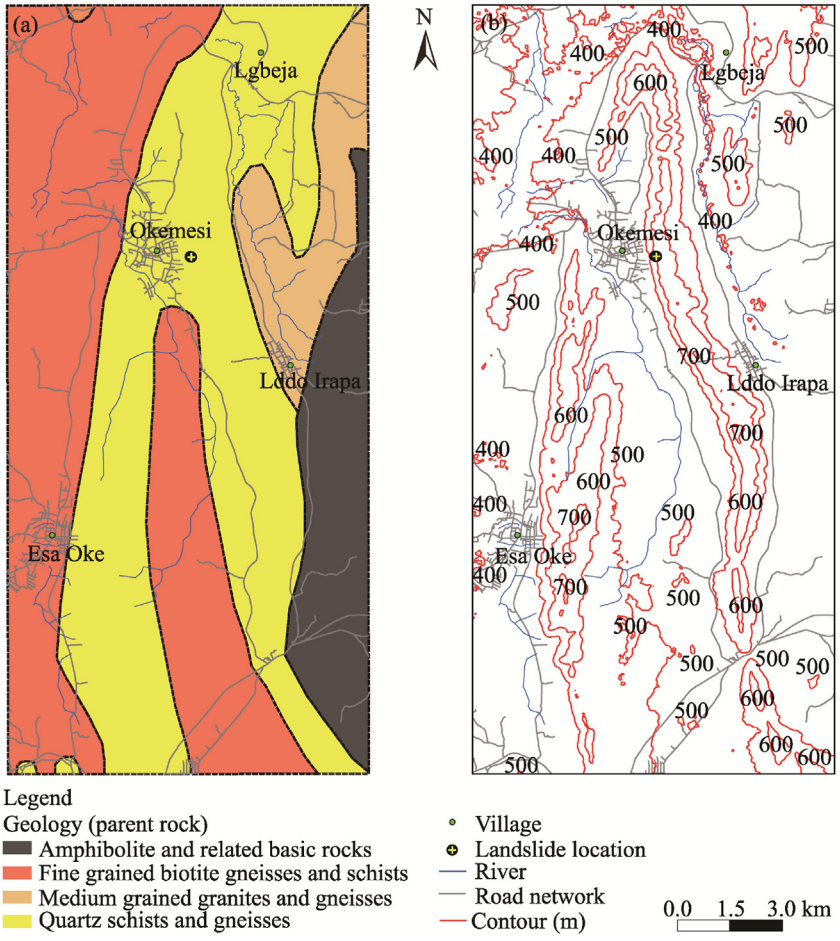

Fig. 2. Distribution of geology (a) and contours (b) of the Okemesi landslide area.

1976; Okunlola and Okoroafor, 2009; Fagbohun et al., 2017; Ayodele, 2020). The Ife-Ilesha schist belt is highly deformed, with visible folding, refolding, fractures, and shear zones. The shear belt that comprises meta-sedimentary, metavolcanite, gneiss, and older granite rocks with shear zones (N–S to NNE–SSW trend), is congruent with the Trans-Saharan Belt's Neoproterozoic Hoggar shear zones (Klemm et al., 1984; Fagbohun et al., 2017).

2.3. Field investigation

Okemesi landslide occurred on 24 September 2017. The landslide has a release area length of 500.0 m and an average length of 200.0 m. While the landslide has an average width of 50.0 m (the horizontal extent of soil and rock movement that occurs downhill during the landslide event), the landslide site has an average depth of 3.0 m and the materials were released during the landslide disaster. This attribute is very critical in determining the volume of materials displaced during the landslide. The horizontal distance of soil and rock movement from the top of the slope to the bottom of the slope is 700.0 m, and the total surface area of the landslide is 8.5 km^2, which is the product of the total length and the average width of the landslide. In addition, the release area (the portion of the slope that actually failed) is 2.5 km^2. The average volume of the landslide is 0.75×10^3 m^3, being the product of the release area and the depth of the slip surface. The volume of materials displaced by the landslide is estimated to be 1144.51 m^3. The slope angles of these displaced residual materials are between 45.00° and 75.00°. The velocity of the landslide was quick but caused no fatalities (Ayodele, 2020). Three soil samples were randomly collected at depths of 0.5 m from three sample points (A, B, and C; Fig. 1) within the Okemesi landslide area. Representative samples of rocks and disturbed soil samples were then retrieved, stored, and appropriately labelled in polyethene bags.

2.4. Data sources and research methods

2.4.1. Data sources

We used both the primary and secondary data in this study. The primary data came from measurements and observations during field investigation, and the secondary data were sourced from the Advanced Land Observing Satellite (ALOS) dataset and a clipped-out Landsat scene of Okemesi and environs. The Okemesi landslide mapping was primarily based on ALOS dataset on 20 August 2007 (provided by the Alaska Facility) and Landsat 8 "Operational Land Imager_Thermal Infrared Sensor (OLI_TIRS)" data on 10 January 2019 (provided by the United States Geological Survey and Earth Science Data Interface). Table 1 presents the various data types and sources.

2.4.2. Grain size analysis

The soil samples from the Okemesi landslide area were sent to Trevi Foundations, a geotechnical company in Nigeria, to classify and determine their engineering properties. For grain size analysis, about 200 g of sub-samples were introduced into a set of stacked sieves, which are fixed to the vibrator. The size of each sieve was measured about 20 min after vibration of the sieve stack. The results were thereafter plotted in order to classify and determine the engineering properties of the displaced slope materials.

2.4.3. Direct shear test

We conducted direct shear test of soil samples in order to determine their shear strength parameters. Specifically, each soil sample was placed in a shear box assemblage of the direct shear machine before normal (vertical) and shear (horizontal) load were applied. The shear, load, and normal displacements were then recorded. The cohesion and angle of the friction were derived from the plot of shear strength and normal stress, respectively. The calculation formula is as follows:

$$q^f = \frac{N_S}{A}, \tag{1}$$

Table 1
Data types and sources.

Item	Type	Date source	Year
Rainfall	Station	Nigerian Meteorological Agency (NiMET) in Ado-Ekiti, Nigeria (https://nimet.gov.ng/https://nimet.gov.ng/)	Monthly rainfall (2001–2017) and daily rainfall (2017)
Landsat image (Landsat 8 OLI_TIRS)	Raster	https://www.usgs.gov/	2019
Copernicus Sentinel data	Raster	Alaska Satellite Facility and National Aeronautics and Space Administration (NASA)	2007
High resolution satellite imagery	Raster	Google Earth Pro	2018
Administrative map	Vector	https://www.usgs.gov/and https://www.nasa.gov/	2010
Geology map	Raster	The Ministry of Agriculture and Natural Resources, Nigeria	1965
Soil map	Raster	Federal Department of Agriculture Land Resources and Soil Survey Division, Nigeria	2018
Study location	Vector point	Field investigation	2019

where, q^f is the quantity of sand; f is the normal stress applied to the soil sample; N_s is the normal displacement (mm); s is the shear strength of the soil sample; and A is the cross-sectional area of the shear box (mm^2). The angle of the friction of slope materials was determined by plotting a graph of N_s against q^f. For sand materials, the angle of the friction usually ranged from 26.00° to 45.00°, increasing with the relative density of compaction.

2.4.4. Collapsibility test

We conducted collapsibility test to find out the possibility of soil collapse in response to different changes in soil water content. The criterion for the evaluation of soil collapsibility proposed by Abelev (1948) was used to conduct the collapsibility test:

$$\delta^z(\%) = \frac{\Delta e}{e_L + 1} \times 100, \tag{2}$$

where, δ^z is the collapsibility coefficient; z is the void ratio during soil saturation; Δe is the void ratio before soil saturation; e_L is the void ratio during saturation; and L refers to the condition of saturation. The value of Δe greater than 2.00% suggests that the material is susceptible to collapse.

Soil collapsibility coefficient is a measure of the susceptibility of soil to significant volume reduction or deformation when subjected to an increase in applied stress. Soil void ratio is the ratio of volume of voids to the volume of solids by the change in applied stress, which represents change in void ratio per unit increase in stress.

2.5. Rainfall analysis

Monthly rainfall data (2001–2017) and daily rainfall data (2017) of the closest synoptic station to the study area were provided by the Nigeria Metrological Agency (NiMET) in Ado-Ekiti, Nigeria. Some of rainfall data were recorded during the first annual peak, which was accompanied by thunderstorms in July, while the others were recorded in September, after a short dry season, often known as the August break. The data were used to analyze rainfall pattern and the influence of daily cumulative rainfall on the triggering of landslide. The study area has a bimodal rainfall pattern that is characterized by high rainfall intensity, frequency, and amount, belonging to the Guinea climatic zone.

2.6. Development of landslide inventory

Previous research usually used landslide inventory to analyze landslide susceptibility, landslide hazard zones, and the various factors that contribute to the occurrence of landslide (Guzzetti et al., 1999). Fig. 3 shows the procedure of drawing landslide vulnerability map. This study used ArcGIS 10.5 software (Environmental Systems Research Institute, Inc., California, the United States) to analyze how environmental factors (such as soil characteristics, geology, land use and land cover type, aspects, curvature, slope, and rainfall distribution) influence landslide. Based on the relationship between landslide and environmental factors, we evaluated these factors by

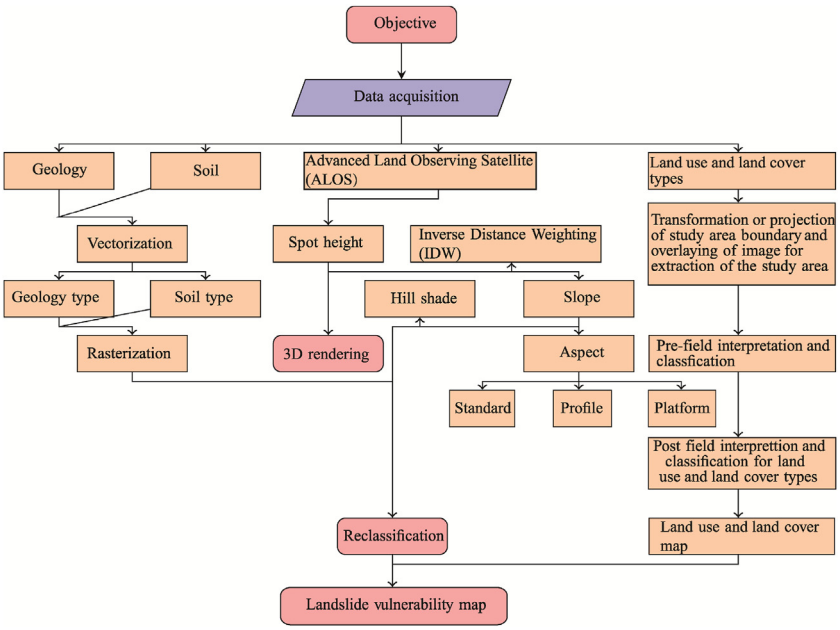

Fig. 3. Flowchart showing the procedure of drawing landslide vulnerability map in Okemesi using remote sensing and GIS technologies.

calculating their weights, and then verified the results and further reclassified them to determine landslide vulnerability. Whatever environmental factors were used, such factors should be operational and measurable (Ayalew and Yamagishi, 2005).

During field investigation, GPS was used to determine and label the location of land use and land cover type, drainage networks and streams locations, in order to develop the landslide susceptibility map. All maps of environmental factors were converted into raster figures with the same coordinate system (Universal Transverse Mercartor Grid System (UTM) zone 31°N).

Fig. 3 shows the assessment flowchart and data inventories used for this study, which included aspect, geology, curvatures, soil characteristics, and metadata. The inventories were also used to analyze landslide susceptibility areas for slope, aspect, altitude, geology, soil texture, distance from lineament, distance from road, and land use and land cover type.

2.6.1. Development of landslide vulnerability map

To generate the hazard susceptible map of the study area, we firstly conducted a vulnerability analysis by constructing a surface representation of the terrain. The 3D grid-based digital model can provide an instant view and nature of the terrain, which was created at 12.5 m intervals and interpolated using ArcScene. Subsequently, using the weighted overlay tool in ArcGIS 10.5 at an influence of 25.00%, we employed an equal percentage influence algorithm (Sun et al., 2023) to weigh and combine each of soil, geology, slope, and land use and land cover type in order to generate the landslide vulnerability map (see Table 2). The terrain map used for the hazard vulnerability analysis was created using the grid-based Digital Elevation Model (DEM). Based on the basic geographical principle that things are closer and more similar, we used inverse distance weighting (IDW) method to interpolate grid-based DEM (Kannan and Singh, 2020).

3. Results and discussion

3.1. Geotechnical analysis

Results of the geotechnical analysis in the Okemesi landslide area are summarized in Table 3. The grain size analysis of the soil in the landslide area showed that the slope materials comprised 17.14% gravel, 59.31% sand, and 19.48% fines. Fig. 4 showed that sand dominated the slope materials and the area can thus be classified as poorly graded gravely sand, which has strong implication for landslide occurrence. The wet density of the soil varied between 2.01 and 2.11 mg/m^3. Stress diagrams of direct shear test of soil samples (A, B, and C) to normal stress at 0.10×10^6, 0.20×10^6, and 0.30×10^6 Pa are also presented in Fig. 4. The poorly graded gravely sand and the reduced low shear strength indicated that the soil in the study area are susceptible to landslide. The high percentage of sand and collapsibility potential in soil sample C indicated a higher risk for slope instability compared to soil samples A and B. Average angles of shearing resistance and cohesion index of the soil were observed to be 17.00° and 0.20×10^3 Pa, respectively. The collapsibility potential of slope materials ranged from 6.65% to 12.62%, showing that the study area has a high to very high potential to occur landslide again.

3.2. Rainfall distribution

Rainfall records in the study area are as presented in Table 4 and Fig. 5. From Fig. 5a we can see that rainfall distribution was unimodal, which is the characteristic of the Guinea climatic zone. The first rainfall peak, with an intensity of 405.7 mm, was recorded in July 2017 (Fig. 5b), which could be due to the destruction of the physical structure of slope materials. Cessation of rainfall in August 2017 was followed by the second peak in September, which initiated the landslide event in this year (2017). Landslide data from Nigerian Meteorological Agency showed that the minimum and maximum rainfall during the landslide occurrence in September were 14.0 and 26.3 mm, respectively. Heavy rainfall in the study area may have saturated soil and rocks while pore water increased in pressure, which might affect the shear strength of soils and initiate the displacement of slope materials. This result aligned with the studies conducted on rainfall-induced landslide by Tran et al. (2018), Dikshit et al. (2019), and Huang et al. (2022).

Table 2
Landslide vulnerability map.

Input parameter	Influence level (%)	Field value	Field class	Weight scale
Land use and land cover type	10.00	1	Farmland	1
		2	Bare or open surface	2
		3	Forest	3
		4	Rock surface	2
		5	Built-up area	3
Reclassified slope	40.00	1	High	1
		2	Medium	2
		3	Low	3
Reclassified geology	25.00	1	High	1
		2	Medium	2
		3	Low	3
Reclassified soil	25.00	1	High	1
		2	Medium	2
		3	Low	3

Table 3
Geotechnical analysis of slope materials.

Attribute	Soil sample		
	A	B	C
Gravel (%)	23.00	0.26	0.03
Sand (%)	0.65	0.57	0.57
Fines (%)	0.12	0.18	0.28
Particle density (mg/m^3)	2.68	2.72	2.67
Natural water content (%)	7.67	5.92	10.95
Wet density (mg/m^3)	2.03	2.11	2.01
Unit weight (kg/m^2)	1989	2068	1970
Collapsibility potential (%)	6.65	12.09	12.62
Direct shear test	0.20	0.25	0.16
Cohesion ($\times 10^3$ Pa)	16.00	18.00	17.00

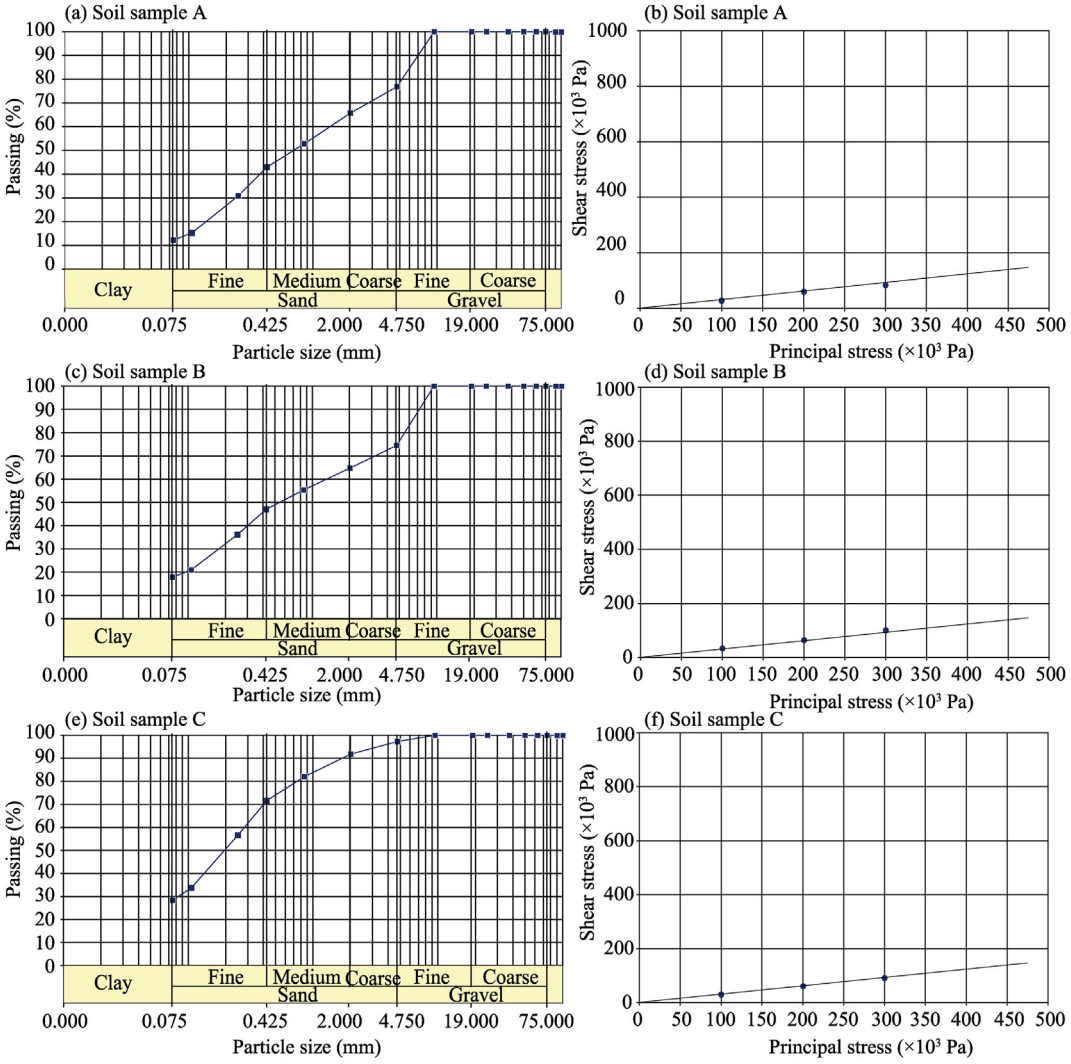

Fig. 4. Grain size distribution of soil samples A (a), B (c), and C (e) and direct shear plot of soil samples A (d), B (e), and C (f).

3.3. Topographic characteristics

The slope of the study area was from 0.00° to 49.00° (Fig. 6a), which was in line with the research of Nseka et al. (2019) and Wang et al. (2020). The map of slope aspect in the study area is presented in Fig. 6b. Regions around the study area registered slope directions

of approximately south (157.51°–202.50°), southwest (202.51°–207.50°), west (247.51°–292.50°), and north (0.00°–22.50° and 337.51°–360.00°), while the highlands were mainly bounded by slope directions of north (0.00°–22.50° and 337.51°–360.00°), northeast (22.51°–67.50°), east (67.51°–112.50°), and southeast (112.51°–157.50°), indicating that the movement of slope materials would follow these directions. Slope aspect showed that majority of flow movement is along the south, southwest, and west directions, accounting for over 80.00% of the total slope aspect.

The slope is indicated by the profile curvature which runs parallel to the slope. This study used IDW to interpolate grid-based DEM in the Okemesi landslide area, which ranged from 374.87 to 726.12 m a.s.l. (Fig. 7a). Fig. 7b showed that the highest profile curvature class was 2.14, while the lowest was −1.30. The positive profile curvature value indicated that the surface was upwardly concave and material flowed and accelerated along such gradient area. Hence, the higher the positive profile curvature value of the area, the higher the probability of a landslide occurrence, while the lower negative profile curvature value of the area, the lower the probability of a landslide occurrence (Mersha and Meten, 2020; Wubalem, 2021).

3.4. Land use and land cover type

The total area of the Okemesi landslide area is 22,441.84 hm^2. The land use and land cover type in 2018 is presented in Table 5 and Fig. 8a. Table 5 showed the area of land use and land cover type. The widespread distribution of farmland within the study area indicated that there are significant human factors in the study area, which increases the likelihood of landslides occurring. This association arises from the positive relationship between more human activities in land exploitation and land cover changes and the increased likelihood of landslip accident (Efiong et al., 2021). The increase in vegetation caused by human activities enhanced the likelihood and probability of slope damage (Efiong et al., 2021; Singh, 2023).

3.5. Landslide vulnerability zones

As shown in Fig. 8b and Table 6, we classified the Okemesi landslide area into high, medium, and low vulnerability zones, with areas of 1345.35, 17,396.33, and 3700.16 hm^2, respectively. From Table 6 we can see that the area percentage of low vulnerability zone was about 29.20% of the total Okemesi landslide area, while the medium vulnerability zone occupied 61.80% and the high vulnerability zone accounted for 9.00%. These medium and high vulnerability zones indicated that there is a high probability of landslide occurrence in the future, and the result are helpful in effectively predicting future landslide in the study area (Huang et al., 2015).

The spatial distribution of landslide vulnerability zones of the study area has implications in understanding future landslide occurrence. As shown in Table 6, the top of ridges (including rock surface) and hills (an area of 2016.25 hm^2, accounting for 8.98% of the steep slope area) in the study area have higher vulnerability. The bare or open surface locating at about 500 m and above, and between 17.00° and 48.00° slope was the high vulnerability zone for landslide occurrence. If landslide occurs in the future, it will affect human activity located downhill. About 17,396.33 hm^2 of land within the study area falls within the medium vulnerability zone for landslide. In this zone, rock materials from high vulnerability zone typically tilt downwards, accelerating their speed and damaging obstacles during the process of tilting downwards. The western part of the Okemesi Town is close to the foot of the ridge, and if a landslide occurs in the area, it will pose a threat to residents there. As observed in Table 6, the low vulnerability zone was 3700.16 hm^2 (29.20%) and distributed in the northern part of the study area and in the valley between Esa Oke and Iddo Irapada. These regions are essential plains that with no hills or ridges and forestland with the slope of less than 5.00°, free from the threat of landslip or rock fall.

Table 4
Statistical description of rainfall in Okemesi landslide area from 2010 to 2017.

Year	Maximum (mm)	Minimum (mm)	Mean monthly (mm)	Annual (mm)	Standard deviation (mm)
2000	214.9	2.4	102.0	1223.6	72.9
2001	217.7	0.0	92.6	1110.7	94.5
2002	279.9	0.0	134.1	1609.8	99.2
2003	335.2	0.0	123.1	1477.1	100.4
2004	275.5	0.0	74.6	895.4	86.3
2005	242.6	0.0	110.0	1320.1	71.5
2006	228.6	0.0	109.7	1316.9	79.6
2007	182.4	0.0	87.6	1051.6	61.8
2008	241.7	0.0	112.3	1347.9	85.2
2009	315.9	0.0	121.4	1456.6	91.9
2010	279.1	0.0	116.5	1397.8	79.6
2011	325.0	0.0	126.1	1512.8	95.1
2012	329.2	6.7	133.8	1605.4	102.6
2013	339.8	15.1	132.6	1591.7	105.9
2014	292.6	0.2	130.5	1566.2	94.7
2015	258.5	0.0	94.5	1133.6	85.3
2016	228.6	0.0	100.2	1201.9	80.2
2017	405.7	0.4	118.3	1419.4	129.1

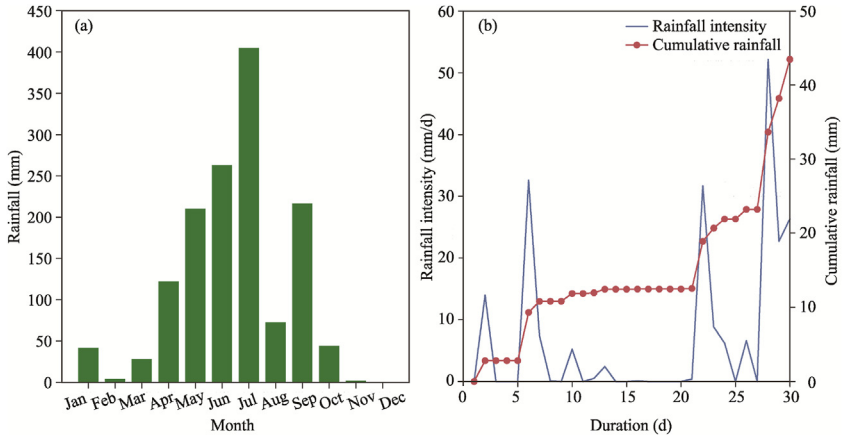

Fig. 5. Monthly rainfall in 2017 (a) and daily rainfall intensity and cumulative rainfall in September 2017 (b) in the Okemesi landslide area.

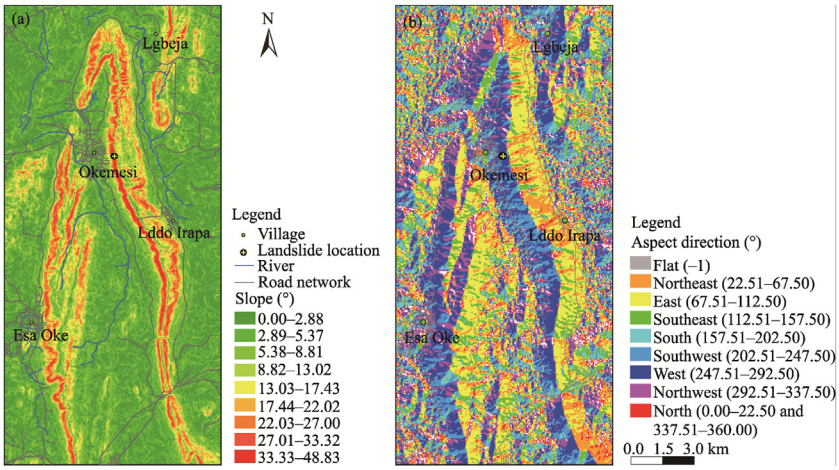

Fig. 6. Spatial distribution of slope (a) and slope aspect (b) in the Okemesi landslide area.

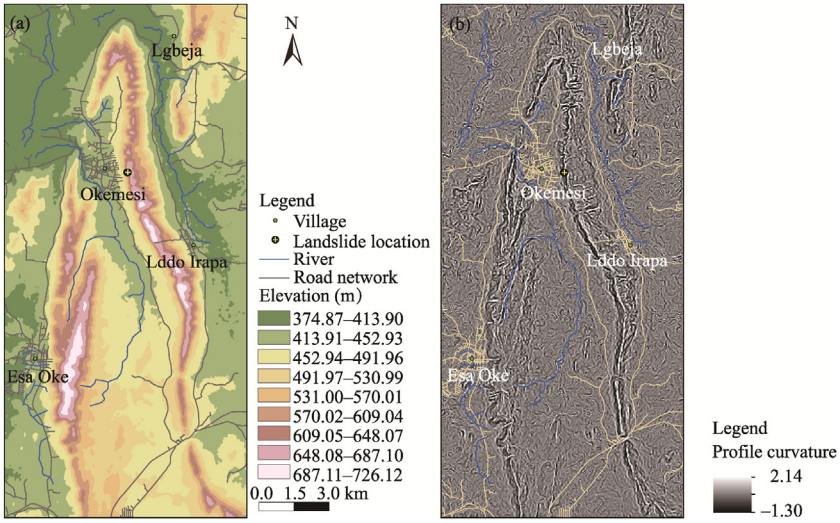

Fig. 7. Spatial distribution of elevation derived from the Inverse Distant Weighting (IDW) (a) and profile curvature (b) in the Okemesi landslide area.

Table 5
Land use and land cover type in 2018 in the Okemesi landslide area.

Type	Area (hm^2)	Proportion (%)
Built-up area	257.18	1.15
Bare or open surface	2695.69	12.01
Forest	7947.56	35.41
Farmland	8898.34	39.65
Rock surface	2643.06	11.78
Total	22,441.83	100.00

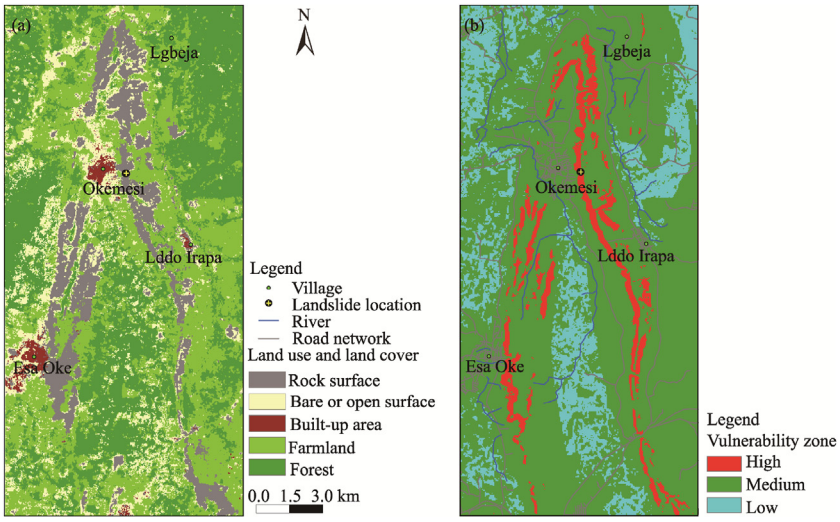

Fig. 8. Distribution of land use and land cover type (a) and landslide vulnerability zone (b) in the Okemesi landslide area.

Table 6
Area and percentage of landslide vulnerability zones in the Okemesi landslide area.

Vulnerability zone	Area (hm^2)	Area percentage (%)
High	1345.35	9.00
Medium	17,396.33	61.80
Low	3700.16	29.20
Total	22,441.84	100.00

4. Conclusions

Studying landslide prone area is the first step in proffering solutions and averting landslide occurrence. In this study, we analyzed various environmental factors to determine the causative factors of the Okemesi landslide. Geotechnical analysis of grain size in the soil showed that the Okemesi landslide area comprised 17.14% gravel, 59.31% sand, and 19.48% fines, with soil wet density varying between 2.01 and 2.11 mg/m^3, thus, the soil type in the Okemesi landslide area can be classified as poorly graded gravely sand. Average angle of shearing resistance and cohesion index of the soil was 17.00° and 0.20 × 10^3 Pa, respectively. The Okemesi landslide was caused by excessive rainfall infiltration into the soil subsurface, which increased pore pressure, thereby leading to a reduction in the effective shear strength of the soil. Slope of the Okemesi landslide area was low, with most of the area recording the slope less than 8.00°. Regions around the study area registered slope directions of approximately south (157.51°–202.5°), southwest (202.51°–247.50°), west (247.51°–292.50°), and north (0.00°–22.50° and 337.51°–360.00°), while the highlands were mainly bounded by slope of north (0.00°–22.50° and 337.51°–360.00°), north east (22.51°–67.50°), east (67.51°–112.50°), and south east (112.51°–157.50°). Spatial distribution of land use and land cover types showed that built-up area, bare or open surface, forest, farmland, and rock surface occupied 1.15%12.01%, 35.41%, 39.65%, and 12.00% of the total study area, respectively. With the vulnerability analysis of landslide, the study area can be classified into high, medium, and low vulnerability zones, with the area percentages of 9.00%, 61.80% and 29.20%, respectively.

The results of this research will provide reference information for the studies of past, present, and future landslide occurrence in the study area. This study will also help decision-makers prioritize sustainable land use and planning, early warning systems, infrastructure investment, and protection of natural resources when formulating measures and regulations to reduce the risk of landslide.

Authorship contribution statement

Oluwakemi Bolanle Akintan: data curation, writing, and editing. Johnson Adedeji Olusola: conceptualization, methodology, editing, and writing review. Olaniyi Patrick Imole: data analysis and writing review. Moyosoluwa Odunayo Adeyemi: data analysis, reviewing, and editing.

Declaration of competing interest

The authors declare that they have no known competing financial interests or personal relationships that could have appeared to influence the work reported in this paper.

Acknowledgements

The authors appreciate the Tertiary Education Fund (TETFUND), Nigeria, for funding this project.

References

Abelev, Y., 1948. The Essentials of Designing and Building on Microporous Soils, vol. 10. Stroitel Naya Promyshelmast, Moskva.
Ayalew, L., Yamagishi, H., 2005. The application of GIS-based logistic regression for landslide susceptibility mapping in the Kakuda-Yahiko Mountains, Central Gapan. Geomorphology 65 (1–2), 15–31.
Ayodele, O., Odeyemi, I., 2010. Analysis of the lineaments extracted from Landsat image of the area around Okemesi, south-western Nigeria. Indian J. Sci. Technol. 3 (1), 31–36.
Ayodele, G.O., 2020. Geological assessment of landslide occurrences in Okemesi area, southwestern Nigeria. Am. J. Environ. Eng. 10 (1), 13–19.
Bamisaiye, O., 2019. Landslide in parts of southwestern Nigeria. SN Appl. Sci. 1, 1–12.
Brand, E.W., Premchitt, J., Phillipson, H., 1984. Relationship between rainfall and landslides in Hong Kong. In: Proceedings of the 4th International Symposium on Landslides. Canadian Geotechnical Society, Toronto, Canada.
Bujang, B., Faisal, H., David, H., et al., 2008. Landslides in Malaysia: Occurrences, Assessment, Analysis and Remediation. Penerbitan Universiti Putra Malaysia, Putrajaya, pp. 406–421.
Chauhan, S., Sharma, M., Arora, M.K., et al., 2010. Landslide susceptibility zonation through ratings derived from artificial neural network. Int. J. Appl. Earth Observ. Conform. 12 (5), 340–350.
Coe, J.A., 2017. Landslide hazards and climate change: a perspective from the United States. In: Ken, H. (Ed.), Slope Safety Preparedness for Impact of Climate Change. CRC Press, Leiden, pp. 479–523.
Dikshit, A., Satyam, N., Pradhan, B., 2019. Estimation of rainfall-induced landslides using the TRIGRS model. Earth Syst. Environ. 3, 575–584.
Efiong, J., Eni, D.I., Obiefuna, J.N., et al., 2021. Geospatial modelling of landslide susceptibility in cross river state of Nigeria. Sci. Afr. 14. https://doi.org/10.1016/j.sciaf.2021.e01032.
Fagbohun, B.J., Adeoti, B., Aladejana, O.O., 2017. Litho-structural analysis of eastern part of Ilesha schist belt, Southwestern Nigeria. J. Afr. Earth Sci. 133, 123–137.
Gbadebo, A.M., Adeyemi, M.O., Adedeji, H.O., et al., 2021. Geotechnical and geomorphological investigation of rainfall induced shallow landslide at Okeigbo, Ondo State, Southwestern Nigeria. J. Afr. Earth Sci. 178. https://doi.org/10.1016/j.jafrearsci.2021.104163.
Guzzetti, F., Carrara, A., Cardinali, M., et al., 1999. Landslide hazard evaluation: a review of current techniques and their application in a multi-scale study, Central Italy. Geomorphology 31 (1–4), 181–216.
Huang, F.M., Chen, J.W., Liu, W.P., et al., 2022. Regional rainfall-induced landslide hazard warning based on landslide susceptibility mapping and a critical rainfall threshold. Geomorphology 408. https://doi.org/10.1016/j.geomorph.2022.108236.
Huang, J., Ju, N.P., Liao, Y.J., et al., 2015. Determination of rainfall thresholds for shallow landslides by a probabilistic and empirical method. Nat. Hazards Earth Syst. Sci. Dis. 15 (12), 2715–2723.
Ige, O.O., Oyeleke, T.A., Baiyegunhi, C., et al., 2016. Liquefaction, landslide and slope stability analyses of soils: a case study of soils from part of Kwara, Kogi and Anambra States of Nigeria. Nat. Hazards Earth Syst. Sci. Dis. 1–39.
Igwe, O., 2015. The geotechnical characteristics of landslides on the sedimentary and metamorphic terrains of south-east Nigeria, West Africa. Geoenviron. Disasters 2, 1–14.
Igwe, O., Una, C.O., 2019. Landslide impacts and management in Nanka area, Southeast Nigeria. Geoenviron. Disasters 6, 1–12.
Kannan, M., Singh, M., 2020. Identifying crime hot spots. In: Chainey, S., Ratcliffe, J. (Eds.), Geographical Information System and Crime Mapping. CRC Press, Leiden, pp. 95–118.
Klemm, D.D., Schneider, W., Wagner, B., 1984. The Precambrian met volcano-sedimentary sequence east of Ife and Ilesha/SW Nigeria. A Nigerian "greenstone belt". J. Afr. Earth Sci. 2 (2), 161–176.
Lee, S., 2019. Current and future status of GIS-based landslide susceptibility mapping: a literature review. Korean J. Remote Sens. 35 (1), 179–193.
Mersha, T., Meten, M., 2020. GIS-based landslide susceptibility mapping and assessment using bivariate statistical methods in Simada area, Northwestern Ethiopia. Geoenviron. Disasters 7 (1), 1–22.
Msilimba, G.G., Holmes, P.J., 2005. A landslide hazard assessment and vulnerability appraisal procedure: Vunguvungu/Banga catchment, Northern Malawi. Nat. Hazards 34, 199–216.
Nseka, D., Kakembo, V., Bamutaze, Y., et al., 2019. Analysis of topographic parameters underpinning landslide occurrence in Kigezi highlands of southwestern Uganda. Nat. Hazards 99 (2), 973–989.
National Population Commission of Nigeria, 2016. Nigeria population and Housing Census 2006 [2023-6-28]. https://ghdx.healthdata.org/record/nigeria-population-and-housing-census-2006.
Ohlmacher, G.C., 2007. Plan curvature and landslide probability in regions dominated by earth flows and earth slides. Eng. Geol. 91 (2–4), 117–134.
Okunlola, O.A., Okoroafor, R.E., 2009. Geochemical and petrogenetic features of schistose rocks of the Okemesi fold belt, Southwestern Nigeria. RMZ Mater. Geoenviron 56 (2), 148–162.
Rahaman, M., 1976. Review of the Basement Geology of South-Western Nigeria. Elizabethan Publish, Lagos, pp. 41–58.
Singh, S.K., 2023. Influence of anthropogenic activities on landslide susceptibility: a case study in Solan district, Himachal Pradesh, India. J. Mt. Sci. 20 (2), 429–447.
Sun, D., Chen, D., Zhang, J., Mi, C., Gu, et al., 2023. Landslide susceptibility mapping based on interpretable machine learning from the perspective of geomorphological differentiation. Land 12 (5), 1018.

Tran, T.V., Alvioli, M., Lee, G., et al., 2018. Three-dimensional, time-dependent modeling of rainfall-induced landslides over a digital landscape: a case study. Landslides 15, 1071–1084.
Wang, K., Xu, H., Zhang, S.J., et al., 2020. Identification and extraction of geomorphological features of landslides using slope units for landslide analysis. ISPRS Int. J. Geo-Inf. 9 (4), 274. https://doi.org/10.3390/ijgi9040274.
Wubalem, A., 2021. Landslide susceptibility mapping using statistical methods in Uatzau catchment area, Northwestern Ethiopia. Geoenviron. Disasters 8 (1), 1. https://doi.org/10.1186/s40677-020-00170-y.